East European Journal of Physics. **3.** 249-258 (2025)
DOI:10.26565/2312-4334-2025-3-22 ISSN 2312-4334

INFLUENCE OF THERMAL RADIATION EFFECT ON MHD MASS TRANSFER FLOW PAST A POROUS VERTICAL PLATE IN PRESENCE OF CONSTANT HEAT FLUX

T.K. Chutia[a], K. Choudhury[b]*, K. Chamuah[a], S. Ahmed[b]
[a]*Department of Mathematics, Moridhal College, Assam, India*
[b]*Department of Mathematics, University of Science & Technology Meghalaya, India*
**Corresponding Author E-mail: kangkan22@gmail.com*
Received June 22, 2025; revised August 18, 2025; accepted August 20, 2025

In this work, we have undertaken to study heat and mass transfer in MHD convective flow past an infinite plate with porous media in existence of radiation, thermal diffusion effect and heat sink. A uniform strength of magnetic field was used transversely in the fluid region. The novelty of this study is to look into the effect of radiation (Rosseland approximation) and heat sink on natural convective flow in the presence of viscous dissipation and Joule heating with constant heat flux and constant suction velocity, past a continuously moving vertical plate in a porous medium. The principal equations are solved by perturbation technique to get statements for velocity, temperature, and concentration fields. In this paper we also consider several physical quantities on the flow domain graphically as well as tabularly which have been studied previously by other researchers except few new cases like light velocity and temperature relationship from different sources such as density gradient effect which are being discussed herein for first time. However, the current investigation has a wide impact on several engineering processes like glass blowing, paper production, extrusion of plastic sheets, etc.
Keywords: *MHD; Heat transfer; Thermal diffusion; Porous media; Thermal radiation*
AMS subject classification: 76W05
PACS: 44.25.+f

INTRODUCTION

The magnetic field strength is often enhanced by a progressive, stable, and sustained current. In this case, considering that a spacecraft must navigate through these regions, which are known to be difficult to navigate, it is important to be able to predict their trajectories. The elements of any spacecraft designed for Mars missions include ion thrusters, attitude control systems (or gyros), power generation and transmission systems, vehicle components such as avionics or sensors etc. Consequently, spacecraft design must take into account the effects of MHD so that controllers can achieve advantageous performance before reaching Mars. Some of them are like Alfven (1942), Ahmed and Choudhury (2019), Seth et al. (2016), Mansour (1990), Seth et al. (2011), Choudhury and Agarwalla (2023), Saikia et al. (2024), Choudhury et al. (2022), Prasad et al. (2023), Balamurugan et al. (2022) etc. Thermal radiation is known to dramatically affect the characteristics of MHD flow. It is a type of electromagnetic wave that has characteristics similar to visible light for its intensity and wavelength but cannot be seen with the naked eye. Thermal radiation can carry energy as heat, infrared, ultraviolet, and X-rays. This induces electric currents in conductors, which generate heat by Joule heating. MHD flow in a viscous incompressible fluid past an impulsively started oscillating plate has been investigated by Appidi et al. (2021). The temperature gradient and stress distributions were computed for different values of space angle of the plates in order to determine the effect of radiation on the MHD flow. They found that both thermal radiation and heat source effect MHD flow and that their effects depend on their spatial distribution at the interface between two media.

The Soret effect or thermal-diffusion effect is an experimental study of the pressure drop under temperature gradient from the solid surface to the fluid. It was originated by the renowned chemist Charles Soret in 1879. The Soret effect is utilized for isotope separation and in mixtures of gases with a very light molecular weight, like H_2 and He. Wide-ranging literature on various features of thermal diffusion on mass transfer related problems can be found in Kafousias and Williams (1998), Ahmed et al. (2013, 2018, 2021), Ahmed and Sengupta (2011), and Chamuah and Ahmad (2021).

The present work generalizes the work done by Chamuah and Ahmed (2021) by including heat sink in MHD convective flow through a porous media. The novelty of this study is to look into the effect of radiation (Rosseland approximation) and heat sink on natural convective flow in the presence of viscous dissipation and Joule heating with constant heat flux and constant suction velocity, past a continuously moving vertical plate in a porous medium. Heat transfer and mass transfer are governed by the same equations, however they different forms. We can rewrite these equations in a simpler way where similarity parameters are used to get rid of their dimensionality. Perturbation techniques are applied to solve these equations and graphically results on plots and tables are shown. However, a comparison with an already published paper has been shown to ensure the accuracy of our present work.

BASIC EQUATIONS

The vector equations that describe the motion of an incompressible viscous electrically conducting Newtonian fluid through the porous medium are:

Cite as: T.K. Chutia, K. Choudhury, K. Chamuah, S. Ahmed, East Eur. J. Phys. 3, 249 (2025), https://doi.org/10.26565/2312-4334-2025-3-22

Equation of continuity:

$$\vec{\nabla}\cdot\vec{q}=0 \tag{1}$$

Gauss's law of magnetism:

$$\vec{\nabla}.\vec{B}=0 \tag{2}$$

Ohm's law:

$$\vec{J}=\sigma(\vec{E}+\vec{q}\times\vec{B}) \tag{3}$$

Momentum equation:

$$\rho(\vec{q}.\vec{\nabla})\vec{q}=\rho\vec{g}-\vec{\nabla}p+\vec{J}\times\vec{B}+\mu\nabla^2\vec{q}-\frac{\mu\vec{q}}{K'} \tag{4}$$

Energy equation:

$$\rho C_p(\vec{q}.\vec{\nabla})T=\kappa\nabla^2T+\varphi+\frac{\vec{J}^2}{\sigma}-Q'(T-T_\infty)-\vec{\nabla}.\vec{q}_r \tag{5}$$

Species continuity equation:

$$(\vec{q}.\vec{\nabla})C=D_M\nabla^2C+\frac{D_MK_T}{T_M}\nabla^2T \tag{6}$$

Equation of state

$$\rho_\infty=\rho\left[1+\beta(T-T_\infty)+\overline{\beta}(C-C_\infty)\right] \tag{7}$$

Radiation heat flux as per Rosseland approximation

$$\vec{q}_r=-\frac{4\sigma^*}{3\kappa^*}\vec{\nabla}T^4 \tag{8}$$

All the physical quantities are defined in the nomenclature.

MATHEMATICAL FORMULATION

The convective flow through a porous vertical plate with uniform suction is investigated by considering the two-dimensional motion of an incompressible fluid. The investigation is based on the following basic premises:

1. Entire fluid properties without density are constant.
2. Plate is electrically insulated.
3. No peripheral electric field is functional to system.
4. Electric potential needed to create Lorentz force be zero.
5. Magnetic field induced by conducting wire parallel to z direction.

We now introduce a Cartesian coordinate system (x',y',z') with X - axis along with the plate in the upward vertical direction, Y - axis normal to the plate directed into the fluid region, and Z - axis along the width of the plate and the induced magnetic field is negligible. The prototype of the problem is shown in Figure A.

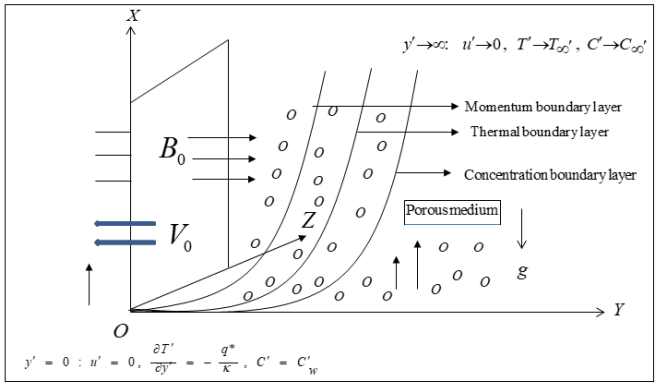

Figure A. Physical model of the problem

The rate of radiative heat flux in an optically thin gray gas is given by

$$\frac{\partial q_r^*}{\partial y'} = -\frac{16\sigma^* T_\infty'^3}{3k^*}\frac{\partial^2 T'}{\partial y'^2} \tag{9}$$

Where k^* and σ^* be respectively absorption coefficient and Stefan-Boltzmann constant.

Based on the preceding axioms, and the usual boundary layer estimates, the governing equations yield the forms as follows:

$$\frac{\partial v'}{\partial y'} = 0 \tag{10}$$

$$v'\frac{\partial u'}{\partial y'} = g\beta\left(T' - T_\infty'\right) + g\overline{\beta}\left(C' - C_\infty'\right) + \nu\frac{\partial^2 u'}{\partial y'^2} - \frac{\sigma B_o^2 u'}{\rho} - \frac{\nu u'}{K'} \tag{11}$$

$$\rho C_P v'\frac{\partial T'}{\partial y'} = \kappa\frac{\partial^2 T'}{\partial y'^2} + \mu\left(\frac{\partial u'}{\partial y'}\right)^2 + \sigma B_O^2 u'^2 - \frac{\partial q_r'}{\partial y'} - Q'\left(T' - T_\infty'\right) \tag{12}$$

$$v'\frac{\partial C'}{\partial y'} = D_M\frac{\partial^2 C'}{\partial y'^2} + \frac{D_M K_T}{T_M}\frac{\partial^2 T'}{\partial y'^2} \tag{13}$$

with boundary conditions

$$y' = 0:\ u' = U,\quad \frac{\partial T'}{\partial y'} = -\frac{q^*}{\kappa},\quad C' = C_w' \tag{14}$$

$$y' \to \infty:\ u' \to 0,\quad T' \to T_\infty',\quad C' \to C_\infty' \tag{15}$$

Equation (10) yields $v' =$ a constant $= -V_o\ \ (V_o > 0)$ (16)

Non-dimensional parameters:

$$u = \frac{u'}{U},\ y = \frac{V_o y'}{\upsilon},\theta = \frac{T' - T_\infty'}{\frac{q^*\upsilon}{\kappa V_o}},\ \ \phi = \frac{C' - C_\infty'}{C_w' - C_\infty'},\ Gr = \frac{\upsilon^2 g\beta q^*}{\kappa U V_o^3},\ Ec = \frac{\rho U^2 V_0}{q^*},\ \Pr = \frac{\mu C_P}{\kappa},$$

$$Gm = \frac{g\overline{\beta}\left(C_w' - C_\infty'\right)\upsilon}{UV_o^2},\ Sc = \frac{\upsilon}{D_M},\ \ k_p = \frac{K'V_0^2}{\upsilon^2},\ M = \frac{\sigma B_o^2\upsilon}{\rho V_o^2}, R = \frac{16\upsilon k^*\sigma^* T_\infty'^3}{\rho C_p V_0^2},$$

$$Q = \frac{Q'\upsilon}{\rho C_p V_0^2}, Sr = \frac{D_M K_T q^*}{T_M\kappa V_o\left(C_W' - C_\infty'\right)}$$

Dimensionless governing equations are

$$\frac{d^2u}{dy^2} + \frac{du}{dy} - \xi u = -Gr\theta - Gm\phi \tag{17}$$

$$\frac{d^2\theta}{dy^2} + \lambda_1\frac{d\theta}{dy} - \lambda_2\theta = -Ec\lambda_3 u'^2 - Ec\lambda_4 u^2 \tag{18}$$

$$\frac{d^2\phi}{dy^2} + Sc\frac{d\phi}{dy} = -ScSr\frac{d^2\theta}{dy^2} \tag{19}$$

Where $\xi = M + \frac{1}{k_p}; \lambda_1 = \frac{\Pr}{1+R}; \lambda_2 = \frac{Q\Pr}{1+R}; \lambda_3 = \frac{1}{1+R}; \lambda_4 = \frac{M}{1+R}$

with boundary conditions

$$y = 0: u = 1,\ \frac{d\theta}{dy} = -1,\ \ \phi = 1 \tag{20}$$

$$y \to \infty : u \to 0, \quad \theta \to 0, \quad \phi \to 0 \tag{21}$$

METHOD OF SOLUTION

We assume the solutions to equations (17) to (19) as

$$u = u_o(y) + Ecu_1(y) + O\left(Ec^2\right) \tag{22}$$

$$\theta = \theta_o(y) + Ec\theta_1(y) + O\left(Ec^2\right) \tag{23}$$

$$\phi = \phi_o(y) + Ec\phi_1(y) + O\left(Ec^2\right) \tag{24}$$

Here Ec, the Eckert number $\left(Ec << 1\right)$. By substituting equations (22) to (24) into equations (17) to (19) and equating the coefficient of analogous terms while deserting the terms of $O\left(Ec^2\right)$, the succeeding equations are derived.

$$\frac{d^2u_o}{dy^2} + \frac{du_o}{dy} - \xi u_o = -Gr\theta_o - Gm\phi_o \tag{25}$$

$$\frac{d^2\theta_o}{dy^2} + \lambda_1 \frac{d\theta_o}{dy} - \lambda_2\theta_0 = 0 \tag{26}$$

$$\frac{d^2\phi_o}{dy^2} + Sc\frac{d\phi_o}{dy} = -ScSr\frac{d^2\theta_o}{dy^2} \tag{27}$$

$$\frac{d^2u_1}{dy^2} + \frac{du_1}{dy} - \xi u_1 = -Gr\theta_1 - Gm\phi_1 \tag{28}$$

$$\frac{d^2\theta_1}{dy^2} + \lambda_1 \frac{d\theta_1}{dy} - \lambda_2\theta_1 = -\lambda_3 u_o'^2 - \lambda_4 u_0^2 \tag{29}$$

$$\frac{d^2\phi_1}{dy^2} + Sc\frac{d\phi_1}{dy} = -ScSr\frac{d^2\theta_1}{dy^2} \tag{30}$$

with boundary conditions

$$y = 0 : u_o = 1;\ \theta_o' = -1;\ \phi_0 = 1;\ u_1 = 0;\ \theta_1' = 0;\ \phi_1 = 0; \tag{31}$$

$$y \to \infty :\ u_o \to 0;\ \ \theta_o \to 0;\ \phi_0 \to 0;\ u_1 \to 0;\ \theta_1 \to 0;\ \phi_1 \to 0; \tag{32}$$

Solutions to the equations (25)-(30) under the conditions (31) and (32) are

$$u_o = p_3e^{-p_1y} - p_4e^{-Scy} + p_6e^{-p_5y} \tag{33}$$

$$\theta_o = \frac{1}{p_1}e^{-p_1y} \tag{34}$$

$$\phi_0 = (1-p_2)e^{-Scy} + p_2e^{-p_1y} \tag{35}$$

$$u_1 = p_{27}e^{-p_5y} + p_{21}e^{-p_1y} + p_{22}e^{-2p_1y} + p_{23}e^{-2Scy} + p_{24}e^{-(p_1+p_5)y} + p_{25}e^{-(p_1+Sc)y} - p_{26}e^{-Scy} \tag{36}$$

$$\theta_1 = p_{13}e^{-p_1y} - p_7e^{-2p_5y} - p_8e^{-2p_1y} - p_9e^{-2Scy} - p_{10}e^{-(p_1+p_5)y} + p_{11}e^{-(p_1+Sc)y} + p_{12}e^{-(p_5+Sc)y} \tag{37}$$

$$\phi_1 = p_{20}e^{-Scy} - p_{14}e^{-p_1y} + p_{15}e^{-2p_5y} + p_{16}e^{-2p_1y} + p_{17}e^{-2Scy} + p_{18}e^{-(p_1+p_5)y} - p_{19}e^{-(p_1+Sc)y} \tag{38}$$

where

$$p_1 = \frac{\lambda_1 + \sqrt{\lambda_1^2 + 4\lambda_2}}{2}, p_2 = \frac{ScSr}{Sc - p_1}, p_3 = \frac{\frac{-Gr}{p_1} - p_2Gm}{p_1^2 - p_1 - \xi}, p_4 = \frac{Gm(1-p_2)}{Sc^2 - Sc - \xi}, p_5 = \frac{1+\sqrt{1+4\xi}}{2},$$

$$p_6 = 1 + p_3 + p_4, p_7 = \frac{\lambda_3 p_5^2 p_6^2 + \lambda_4 p_6^2}{4p_5^2 - 2\lambda_1 p_5 - \lambda_2}, p_8 = \frac{\lambda_3 p_1^2 p_3^2 + \lambda_4 p_3^2}{4p_1^2 - 2\lambda_1 p_1 - \lambda_2}, p_9 = \frac{\lambda_3 Sc^2 p_4^2 + \lambda_4 p_4^2}{4Sc^2 - 2\lambda_1 Sc - \lambda_2},$$

$$p_{10}=\frac{2\lambda_3 p_1 p_3 p_5 p_6+2\lambda_4 p_3 p_6}{(p_1+p_5)^2-\lambda_1(p_1+p_5)-\lambda_2}, p_{11}=\frac{2\lambda_3 p_1 p_3 p_4 Sc+2\lambda_4 p_3 p_4}{(p_1+Sc)^2-\lambda_1(p_1+Sc)-\lambda_2},$$
$$p_{12}=\frac{2\lambda_3 p_4 p_5 p_6 Sc+2\lambda_4 p_4 p_6}{(p_5+Sc)^2-\lambda_1(p_5+Sc)-\lambda_2},$$

$$p_{13}=\frac{1}{p_5}[2p_5 p_7+2p_1 p_8+2Scp_9+(p_1+p_5)p_{10}-(p_1+Sc)p_{11}-(p_5+Sc)p_{12}],$$

$$p_{14}=\frac{ScSrp_1^{\,2}p_{13}}{p_1^{\,2}-Scp_1}, p_{15}=\frac{4ScSrp_5^{\,2}p_7}{4p_5^{\,2}-2Scp_5}, p_{16}=\frac{4ScSrp_1^{\,2}p_8}{4p_1^{\,2}-2Scp_1}, p_{17}=\frac{4Sc^3 Srp_9}{2Sc^2},$$

$$p_{18}=\frac{ScSr(p_1+p_5)^2 p_{10}}{(p_1+p_5)^2-Sc(p_1+p_5)}, p_{19}=\frac{ScSr(p_1+Sc)^2 p_{11}}{(p_1+Sc)^2-Sc(p_1+Sc)}, p_{20}=p_{14}-p_{15}-p_{16}-p_{17}-p_{18}+p_{19},$$

$$p_{21}=\frac{Gmp_{14}-Grp_{13}}{p_1^{\,2}-p_1-\xi}, p_{22}=\frac{Grp_8-Gmp_{16}}{4p_1^{\,2}-2p_1-\xi}, p_{23}=\frac{Grp_9-Gmp_{17}}{4Sc^2-2Sc-\xi}, p_{24}=\frac{Grp_{10}-Gmp_{18}}{(p_1+p_5)^2-(p_1+p_5)-\xi},$$

$$p_{25}=\frac{-Grp_{11}+Gmp_{16}}{(p_1+Sc)^2-(p_1+Sc)-\xi}, p_{26}=\frac{Gmp_{20}}{Sc^2-Sc-\xi}, p_{27}=p_{26}-p_{21}-p_{22}-p_{23}-p_{24}-p_{25}$$

Skin friction:
Skin friction is given by

$$\tau=-\left.\frac{\partial u}{\partial y}\right|_{y=0}=-[\tau_0+Ec\tau_1] \tag{39}$$

Where

$$\tau_0=-p_1 p_3+Scp_4-p_5 p_6$$

$$\tau_1=-p_5 p_{27}-p_1 p_{21}-2p_1 p_{22}-2Scp_{23}-(p_5+p_1)p_{24}-(Sc+p_1)p_{25}+Scp_{26}$$

Plate temperature:
The dimensionless temperature field is,

$$\theta(y)=\theta_0(y)+Ec\,\theta_1(y)$$

Non-dimensional plate temperature is given by,

$$\theta_w=\theta_0(0)+Ec\,\theta_1(0) \tag{40}$$

Sherwood number:
Sherwood number is given by

$$Sh=-\left.\frac{\partial\phi}{\partial y}\right|_{y=0}=-[Sh_0+EcSh_1] \tag{41}$$

Where

$$Sh_0=-Sc(1-p_2)-p_1 p_2$$

$$Sh_1=-Scp_{20}+p_1 p_{14}-2p_5 p_{15}-2p_1 p_{16}-2Scp_{17}-(p_1+p_5)p_{18}+(p_1+Sc)p_{19}$$

RESULTS AND DISCUSSIONS

The numerical computations have been carried out for the representative velocity, temperature, concentration, skin friction, and plate temperature at the wall for different values of the physical parameters involved in the problem. The influence the flow parameters Prandtl number, Schmidt number, thermal radiation, Soret number, thermal Grashof number and mass Grashof number on these fields have been depicted in Figures 1 to 15. Numerical results of shear stress and plate temperature are presented in Table 1 and Table 2. The default values for the flow parameters are chosen as

$$\Pr=0.71, Sc=0.6, R=1, K=1, Sr=1, Gr=10, Gm=5, M=1.5, E=0.01, Q=5$$

The drag-like force called Lorentz force produces a kind of friction on the flow and thus opposes the transport phenomenon. With the increasing values of magnetic parameter, the fluid velocity decreases significantly which is seen from Figure 1. This observation implies that applying a transverse magnetic field decelerate fluid motion. This observation is consistent with the physical fact that a magnetic body force develops due to the interaction of the fluid velocity and magnetic field, which serves as a resistive force to the flow, and as a consequence fluid flow gets decelerated. The velocity distribution due to Soret number shows statistical characteristic features in which it can be observed from Figure 2 that with temperature gradients inducing significant mass diffusion effects, the fluid velocity increases. The effect of thermal radiation on flow phenomena is depicted in Figure 3 where it is seen that with increase in thermal radiation rate, decrease in energy transport to fluid takes place and hence decelerates motion of fluid particles. The effect of heat sink on fluid velocity is seen in Figure 4. It has been observed that fluid velocity decreases marginally with small increase in heat sink whereas it decreases significantly with significant rise in heat sink. So, with large amount of heat absorption the fluid motion decreases rapidly. In this portion of the experiment, the effect of Prandtl number and Schmidt number on the velocity profile is discussed.

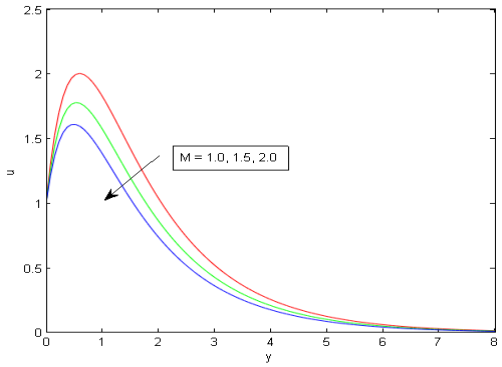

Figure 1. Rate of movement for variations in M

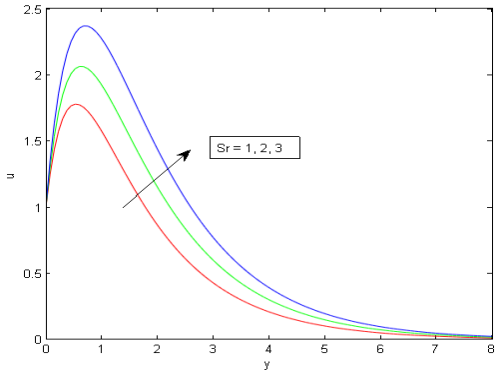

Figure 2. Rate of movement for variations in Sr

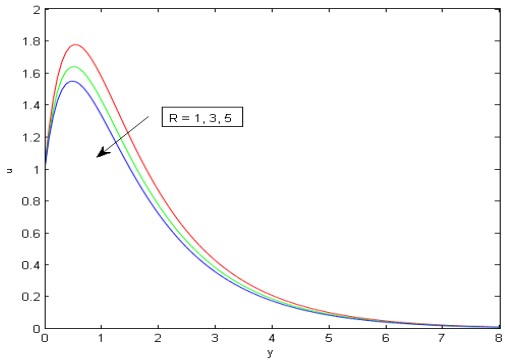

Figure 3. Rate of movement for variations in R

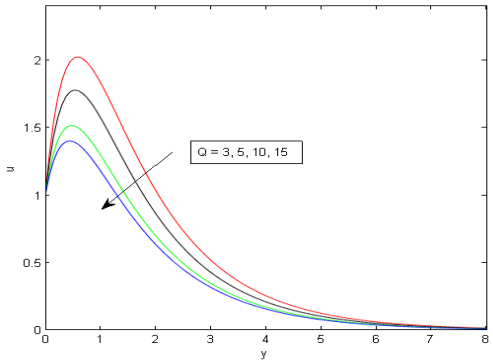

Figure 4. Rate of movement for variations in Q

In Figure 5, it was observed that as the Schmidt number increases, momentum diffusivity increases, resulting in lower fluid velocities. This result was verified by plotting velocity versus Schmidt number in Figure 6, which showed an increase in fluid velocity with increasing values of Prandtl number.

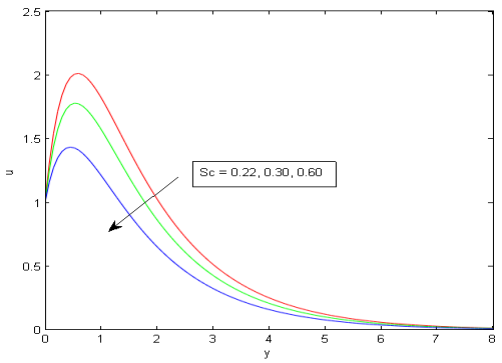

Figure 5. Rate of movement for variations in Sc

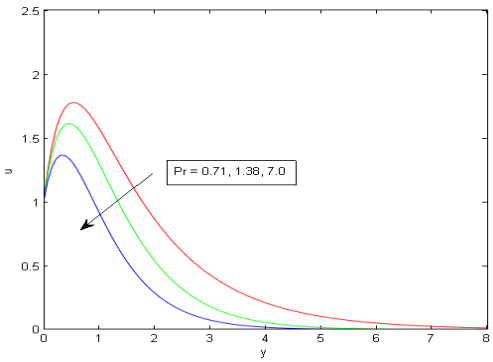

Figure 6. Rate of movement for variations in Pr

The effects of Grashof numbers are depicted in Figures 7 and 8 where it was seen that both thermal buoyancy force and mass buoyancy force have similar effects on the flow domain as well as any one of these forces dominates over another depending upon specific conditions. Thermal buoyancy force (Figure 7) and solutal buoyancy force (Figure 8)

cause the velocity field to rise substantially. This happens due to the direct proportionality of buoyancy force to those of Grashof numbers.

The heat transfer rate of a fluid is controlled by the momentum and thermal insulation of the interface between the fluid and its surroundings. The influence of the heat conductivity on temperature distribution is displayed in Figures 9 and 10. It has been observed that high conductivity fluids such as molten salt have low thermal diffusivity, which results in fast changes in temperatures. Thermal radiation also affects fluid temperature distribution because low thermal conductivity materials absorb large amounts of radiant energy due to higher temperatures compared to fluids having high thermal conductivity. Figure 11 shows another example where fluid temperature can be affected by heat sink coefficient. It is observed from Figure 12 that fluid temperature is reduced due to the increasing values of Eckert number.

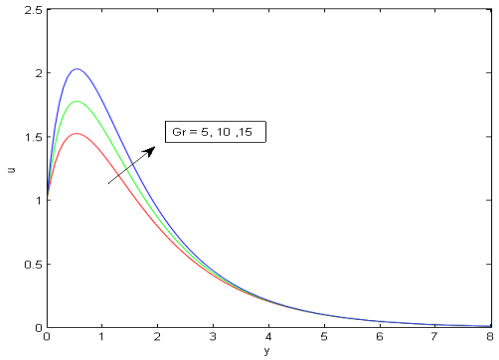

Figure 7. Rate of movement for variations in Gr

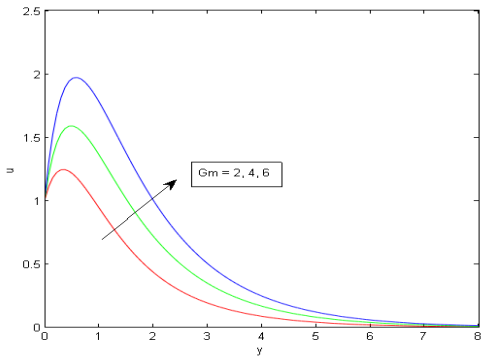

Figure 8. Rate of movement for variations in Gm

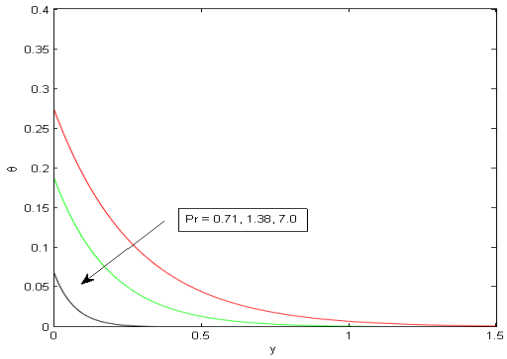

Figure 9. Temperature field for variations in *Pr*

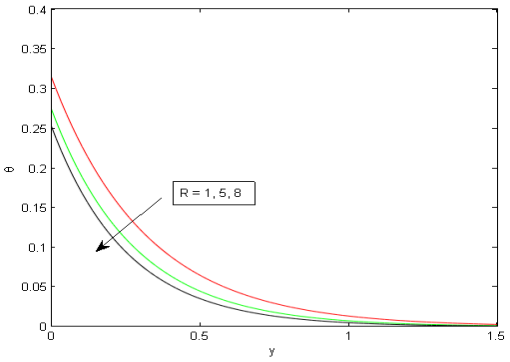

Figure 10. Temperature field for variations in *R*

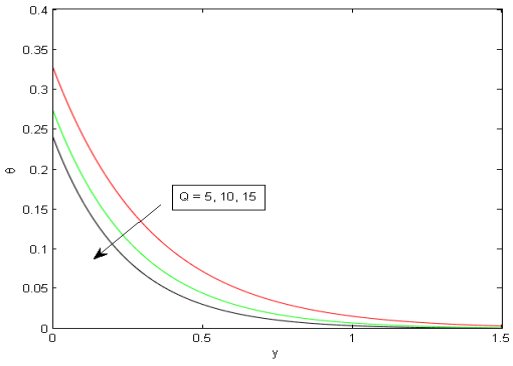

Figure 11. Temperature field for variations in *Q*

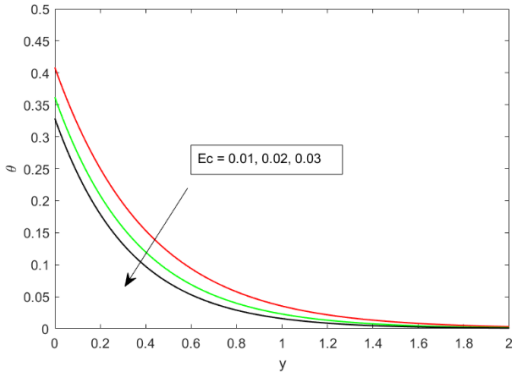

Figure 12. Temperature field for variations in *Ec*

The concentration profiles are plotted in Figures 13, 14 and 15. In Figure 13, it is seen that the concentration of the fluid falls with increasing values of Schmidt number due to low mass diffusivity. It is noted that an increase in Schmidt number means a fall in mass diffusivity. Thus, the concentration on the plate falls because of low mass diffusivity. This observation is compatible with the physical reality that increasing Schmidt number causes a decrease in mass diffusivity, which causes a decrease in fluid concentration. Figure 14 indicates that an increase in Soret n umber leads to an increase in the fluid concentration. Figure 15 shows that the influence of heat sink is to decrease the fluid concentration.

As we can see from Table 1, as R, Sc and Q increase, skin friction increases. In addition to this, it is inferred from Table 1 that the skin friction gets diminished for increasing magnetic parameter M. This indicates that the imposition of a transverse magnetic field inhibits viscous drag due to its application on thin films with high aspect ratio. Henceforth, the coefficient of momentum at the planar surface becomes larger for increasing M. Table 2 shows that plate temperature

increases when Pr increase. The temperature of the plate decreases due to the effect of the magnetic field M as it is applied transversely to the fluid region and the similar effect found for Eckert number Ec.

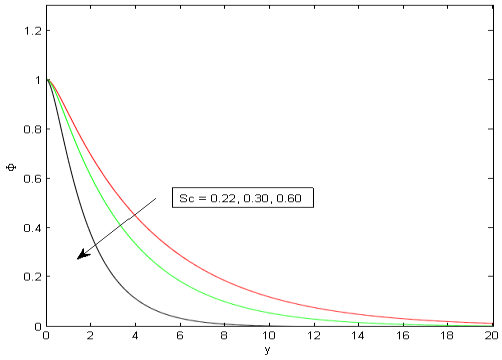

Figure 13. Concentration profile for variations in *Sc*

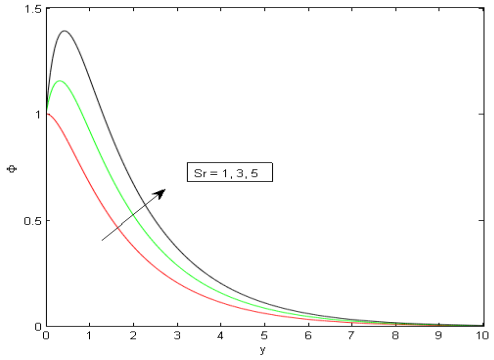

Figure 14. Concentration profile for variations in *Sr*

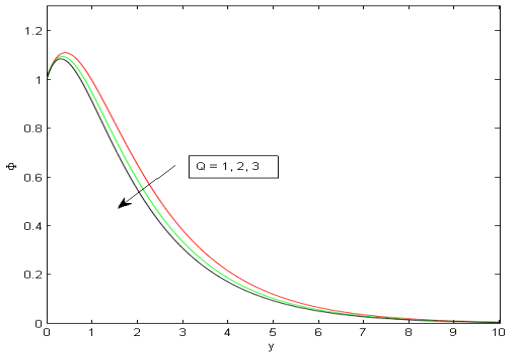

Figure 15. Concentration profile for variations in *Q*

Table 1: Shear stress τ at the plate for the values of $\Pr = 0.71, Sc = 0.6, R = 1, K = 1, Sr = 1, Gr = 10, Gm = 5, M = 1.5, E = 0.01, Q = 5$

Sc	M	R	Q	Sr	τ
0.30	1.5	1	5	1	2.8377
0.60	1.5	1	5	1	7.2121
0.78	1.5	1	5	1	9.3817
0.60	**1**	1	5	1	3.1568
0.60	**2**	1	5	1	2.8376
0.60	**3**	1	5	1	2.1771
0.60	1.5	**2**	5	1	5.3559
0.60	1.5	**3**	5	1	6.1846
0.60	1.5	**5**	5	1	7.2657
0.60	1.5	1	**2**	1	5.5559
0.60	1.5	1	**4**	1	6.7606
0.60	1.5	1	**6**	1	8.3296
0.60	1.5	1	5	**1**	4.2394
0.60	1.5	1	5	**2**	4.6924
0.60	1.5	1	5	**3**	4.8447

Table 2: Plate temperature $\theta(0)$ for changed values of the parameters Pr, M, Ec

Pr	M	Ec	$\theta(0)$
0.71	1	0.01	0.2262
1.38	1	0.01	0.4252
7.0	1	0.01	0.4496
0.71	**1**	0.01	0.2262
0.71	**2**	0.01	0.0540
0.71	**3**	0.01	0.0239
0.71	1	**0.01**	0.2262
0.71	1	**0.02**	0.0540
0.71	1	**0.03**	0.0240

COMPARISON

Figure 16 is plotted to make a comparison of the current work with the previously published result of Chamuah and Ahmed (2021). Figure 16 displays the variations in velocity profile due to radiation, in absence of heat sink i. e., Q=0. Figure 17 (Figure 4 of (2021)) shows the velocity field due to radiation. It is seen that both the figures are identical and indicates a decrease in velocity due to radiation.

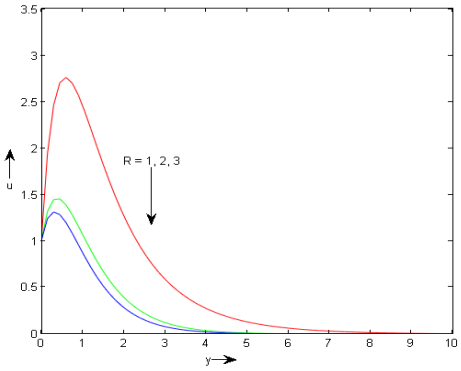

Figure 16. Velocity field for radiation parameter

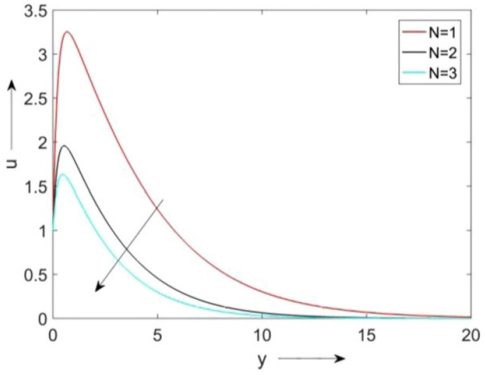

Figure 17: Figure 4 of Chamuah & Ahmed (2021)

CONCLUSIONS

The present study leads to attain at the subsequent conclusions:

1. Fluid velocity diminutions due to imposition of magnetic field and thus magnetic field can be effectively used in controlling the fluid motion.
2. Fluid motion enhances due to thermal Grashof number, mass Grashof number and thermal diffusion while the trend is reversed with the increase in thermal radiation, heat sink and Schmidt number.
3. Temperature of the fluid drops under the influence of Prandtl number, thermal radiation, and heat sink.
4. Concentration of the fluid grows with Soret number whereas it decreases due to heat absorption and Schmidt number.
5. Skin friction at the wall rises for increasing values of Soret number, Schmidt number, radiation, and heat sink parameter. In the other hand, it is reduced due to the application of transverse magnetic field.

List of Symbols

$\vec{q}$	velocity vector	C_∞	free stream concentration
ρ	density, kg/m^3	σ	electrical conductivity, $1/(ohm.m)$
ν	kinematic viscosity, m^2/s	$\vec{E}$	electrical field
$\vec{J}$	current density	β	thermal expression coefficient, $1/k$
$\vec{g}$	acceleration vector	$\overline{\beta}$	solutal expansion coefficient, $1/kmol$
$\vec{B}$	magnetic flux density vector	T_∞	free stream concentration, k
κ	thermal conductivity, $W/m.K$	C_∞	free stream concentration, kmol
κ*	mean absorption coefficient, $1/m$	B_o	applied magnetic field strength, Tesla
φ	energy viscous dissipation per unit volume	μ	viscosity coefficient, kg/ms
p	fluid pressure	θ	non-dimensional temperature
U	velocity of free stream	ϕ	non-dimensional concentration
K	porosity parameter	Pr	Prandtl number
q*	heat flux, W/m^2	Q	heat sink
$\vec{q}_r$	radiation heat flux	Sc	Schmidt number
$\vec{J}^2/\sigma$	energy of ohmic dissipation per unit volume	Gr	thermal Grashof number
T	fluid temperature, K;	M	magnetic parameter
C	concentration, $kmol/m^3$	Gm	solutalGrashof number
C_w	plate species concentration	R	radiation
Ec	Eckert number	Sr	Soret number

ORCID

K. Choudhury, https://orcid.org/0000-0003-2809-8428

REFERENCES

Ahmed, N. "MHD Convection with Soret and Dufour Effects in a Three-Dimensional Flow Past an Infinite Vertical Porous Plate," Can. J. Phys., **88**(9), 663-674 (2010). https://doi.org/10.1139/P10-056

Ahmed, N. & Choudhury, K. "Heat and mass transfer in three-dimensional flow through a porous medium with periodic permeability," Heat transfer Asian research, **48**(2), 644-662 (2019). https://doi.org/10.1002/htj.21399

Ahmed, N. & Dutta, M. "Natural convection in transient MHD dissipative flow past a suddenly started infinite vertical porous plate: A Finite Difference Approach," Heat Transfer Research, **49**(6), 491-508 (2018). https://doi.org/10.1615/HeatTransRes.2018016823

Ahmed, N., Sengupta, S. & Datta, D. "An Exact Analysis for MHD Free Convection Mass Transfer Flow Past an Oscillatory Plate Embedded ina Porous Medium," Chem. Eng. Commun. **200**, 494-513 (2013). https://doi.org/10.1080/00986445.2012.709474

Ahmed, N. & Sengupta, S. "Thermo-diffusion and Diffusion-thermo effects on a Three-Dimensional MHD Mixed Convection Flow Past an Infinite Vertical Porous Plate with Thermal Radiation," Magnetohydrodynamics, **47**(1), 41-60 (2011).

Alfven, H. "Discovery of Alfven waves," Nature, 150, 405-406 (1942).

Appidi, L., B.S. Malga & P.P. Kumar, "Effect of thermal radiation on an unsteady MHD flow over an impulse vertical infinite plate with variant temperature in existence of Hall current, **51**(3), 2367-2382 (2021). https://doi.org/10.1002/htj.22402

Balamurugan, K.S., Varma, N., & Prasad, J.L. "Entropy generation analysis on forced and free convection flow in a vertical porous channel with aligned magnetic field and Navier slip, Heat Transfer, **52**(7), 4619-4639 (2023). https://doi.org/10.1002/htj.22897

Chamuah, K. & Ahmed, N. "MHD free convective dissipative flow past a porous plate in a porous medium in the presence of radiation and thermal diffusion effects," Heat transfer, **51**(2), 1964-1981 (2022). https://doi.org/10.1002/htj.22383

Choudhury, K. & Agarwalla, S. "Hydromagnetic convective flow past a porous vertical plate with constant heat flux and heat sink," Mathematics in Engineering, Science and Aerospace, **14**(2), 579-595 (2023).

Choudhury, K., Agarwalla, S. & Ahmed, N., "Diffusion-thermo effect on MHD dissipative flow past a porous vertical plate through porous media," Heat Transfer, **51**, 6836-6855 (2022). https://doi.org/10.1002/htj.22626

Kafoussias, N. G., & Williams, E.W. "Thermal Diffusion and Diffusion Thermo Effects on Mixed Free Forced Convective and Mass Transfer Boundary Layer Flow with Temperature Dependent Viscosity," Int. J. Eng. Sci., **33**, 1369-1384 (1998). https://doi.org/10.1016/0020-7225(94)00132-4

Mansour, M. A. "Radiation and free convection effects on the oscillatory flow past a moving vertical porous plate," Astrophys. Space Sci., **166**(2), 269-275 (1990). https://doi.org/10.1007/BF01094898

Prasad, JL, Rao, Venkateswara I. V., Balamurugan, KS & Dharmaiah, G. "Radiative Magnetohydrodynamic flow over a vertical cone filled with convective nanofluid," Communications in Mathematics and Applications, **13**(2), 449–459. (2022). https://doi.org/10.26713/cma.v13i2.1795

Saikia, D J, Ahmed, N. & Bordoloi, R. "Natural convective MHD mass transfer flow past an infinite vertical porous plate embedded in a porous medium with thermal diffusion and chemical reaction," Special Topics & Reviews in Porous Media, **14**(2), 63-75 (2023). https://doi.org/10.1615/SpecialTopicsRevPorousMedia.2023045885

Seth, G. S., Ansari, M. S. & Nandkeolyan, R. "MHD Natural convection flow with radiation heat transfer past an impulsively moving plate with ramped temperature," Heat Mass Transfer, **47**, 551-561 (2011). https://doi.org/10.1007/s00231-010-0740-1

Seth, G. S., Sharma, R. & Kumbhakar, B. "Heat and mass transfer effects on unsteady MHD natural convection flow of a chemically reactive and radiating fluid through a porous medium past a moving vertical plate with arbitrary ramped temperature," J. Appl. Fluid Mech., **9**(1), 103-117 (2016). https://doi.org/10.18869/acadpub.jafm.68.224.23961

ВПЛИВ ТЕПЛОВОГО ВИПРОМІНЮВАННЯ НА МГД-МАСООБМІННИЙ ПОТІК ПОВЗ ПОРИСТУ ВЕРТИКАЛЬНУ ПЛАСТИНУ ЗА НАЯВНОСТІ ПОСТІЙНОГО ТЕПЛОВОГО ПОТОКУ

Т.К. Чутія[a], К. Чоудхурі[b], К. Чамуа[a], С. Ахмед[b]

[a]Кафедра математики, Коледж Моріджал, Ассам, Індія

[b]Кафедра математики, Університет науки і технологій Мегхалаї, Індія

У цій роботі ми взялися за вивчення тепло- та масообміну в конвективному потоці МГД повз нескінченну пластину з пористим середовищем за наявності випромінювання, ефекту термодифузії та тепловідведення. Рівномірна напруженість магнітного поля використовувалася поперечно в області рідини. Новизна цього дослідження полягає у вивченні впливу випромінювання (наближення Росселенда) та тепловідведення на природний конвективний потік за наявності в'язкої дисипації та джоулевого нагрівання з постійним тепловим потоком та постійною швидкістю всмоктування повз безперервно рухому вертикальному потоці в пористому середовищі. Основні рівняння розв'язуються методом збурень для отримання формулювань для полів швидкості, температури та концентрації. У цій статті ми також розглядаємо кілька фізичних величин в області потоку графічно, а також таблично, які раніше вивчалися іншими дослідниками, за винятком кількох нових випадків, таких як залежність швидкості світла від температури з різних джерел, таких як ефект градієнта густини, які обговорюються тут вперше. Однак, поточне дослідження має широкий вплив на кілька інженерних процесів, таких як видування скла, виробництво паперу, екструзія пластикових листів тощо.

Ключові слова: *МГД; теплопередача; термодифузія; пористі середовища; теплове випромінювання*